Fabrication of axicons by cw laser effusion

J. M. González-Leal* and J. A. Angel

Department of Condensed Matter Physics, Faculty of Sciences, University of Cadiz, 11510 – Puerto Real (Cadiz), Andalusia, Spain

**Corresponding author: juanmaria.gonzalez@uca.es*

Received February 8, 2007; revised June 26, 2007; accepted June 27, 2007; posted June 29, 2007 (Doc. ID 79936); published August 2, 2007

The fabrication of axicons by cw laser effusion is introduced for the case of a chalcogenide alloy, and experimental results concerning the lateral resolution and the intensity distribution along the optical axis are reported. © 2007 Optical Society of America

OCIS codes: 220.1250, 310.1860.

Laser deposition techniques have been focused traditionally to the use of pulsed laser sources and off-axis target-substrate deposition configurations to grow a number of both superconductor and semiconductor materials for planar technologies [1,2]. Typically, the substrate is placed onto a rotary holder, at distances of the order of centimeters from the starting material, with the evaporation axis and rotation axis being noncoincident, to improve the thickness uniformity of the deposited films. In addition, laser radiation impinges the material at oblique incidence to improve the photon absorption efficiency in the target, in such a fashion that interaction between the light beam and plasma plume is reduced.

We introduce here a laser deposition approach for the fabrication of semiconductor material deposits with optical functionality that, unlike pulsed laser deposition (PLD), uses cw laser sources and on-axis geometry, with target and substrate facing parallel to each other and close to each other, as illustrated in Fig. 1. The aim of the present Letter is to demonstrate the success of this original configuration for the fabrication of axicons and to report preliminary evidence of its performance, as well as the characterization of these particular optical structures, in the particular case of using a chalcogenide alloy as starting material. It is to be highlighted here that the use of axicons, and hence the departure from traditional diffraction-limited beam propagation, is rapidly advancing many applications including confocal imaging and optical trapping [3–8], which, to our mind, support the interest of the present work.

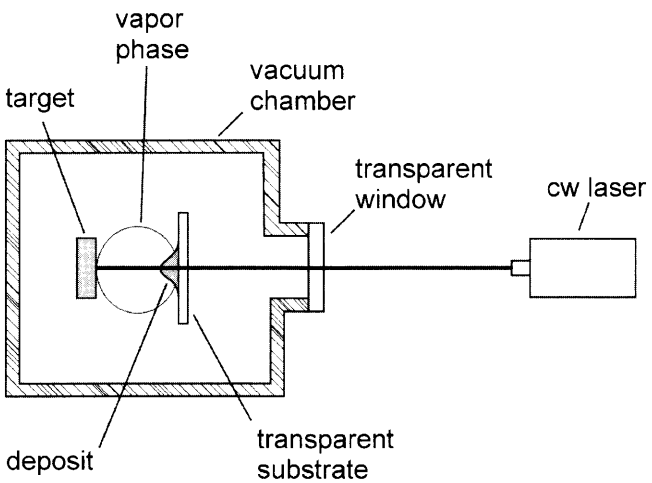

Fig. 1. Sketch of the laser deposition geometry for axicon fabrication.

Samples reported here were fabricated according to the on-axis geometry shown in Fig. 1, using a cw $Nd:YVO_4$ source emitting TEM_{00} laser radiation at $\lambda = 532$ nm wavelength (Coherent, model Verdi V6) and $As_{20}S_{80}$ glass as starting material. This amorphous chalcogenide alloy was originally synthesized in bulk form from their 5*N*-purity constituents by conventional melt quenching in air. Structural and electronic studies of this particular alloy, as well as other composition within the As_xS_{100-x} compositional line, have been previously reported by the authors in [9]. Target material was made in tablet form, 13 mm in diameter and about 1 mm in thickness, from this bulk alloy, and it was synthesized from the glass powder by pressing 125 mg of the starting material at 10 tons for 5 min with the help of a pneumatic press. It has been checked that the absorption of the laser radiation in the target material was improved by the surface roughness of the tablet, in comparison with the effect observed in the specular surface of the bulk. Depositions were performed onto transparent glass substrates (BDH, model Superpremium), in 10^{-5} mbar vacuum, using a collimated laser beam with 4 mm diameter Gaussian cross section at $1/e^2$ intensity. Substrates were placed at 1.9 ± 0.1 mm from the target. Deposited samples were checked to be amorphous by x-ray diffraction (Bruker, model D8 Advanced). No compositional changes were observed between the starting material and the deposits, as evidenced by energy dispersion spectroscopy performed in a scanning electron microscope (FEI, model Quanta 200).

The thickness profile of the deposits was measured with a stylus-based profilometer (Veeco, model Dektak 8), and the one corresponding to a deposit fabricated with 300 mW power and 12 s time is shown in Fig. 2. This deposit was checked to have circular symmetry, and its radial thickness dependence fits the equation

$$t(r) = \frac{A}{[1 + (r/a)^2]^2}, \tag{1}$$

with r being the radial distance to the center of the deposit, A the top thickness at $r = 0$, and a the dis-

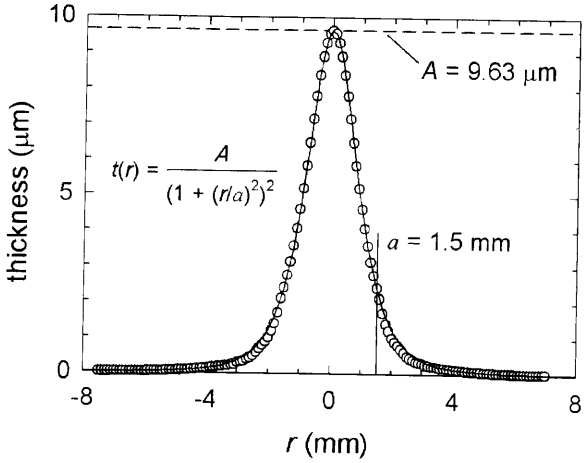

Fig. 2. Experimental thickness data (circles) measured with the profilometer. The solid curve is the theoretical thickness profile for a deposit obtained from a material emission source following the Lambert cosine law. The mathematical function for the thickness profile, $t(r)$, and values for the fitting parameters a and A are indicated.

tance from the effusion source to the substrate. In particular, experimental data of Fig. 2 fit Eq. (1) with $a=1.5$ mm, which agrees with the above-mentioned experimental substrate-target distance of about 1.9 mm. Differences between these values remain to be clarified in the course of the research, which could be related with possible deformations of the target surface due to light-induced heating.

Equation (1) comes from the well-known Lambert cosine law, which rules the mass emission in the effusion process [10]. This emission process verifies in Knudsen cells and also in the so-called Knudsen layers occurring in laser evaporation [11]. The Knudsen layer occurs immediately above the target material and it is widely reported to have a thickness of the order of the molecular mean free path, with typical values of the order of millimeters at high vacuum (10^{-5}–10^{-9} mbar).

The analysis of the optical field through along the optical axis for the profile given in Eq. (1) has been developed by one of the authors under the assumptions of a homogeneous dielectric material with refractive index n, an input Gaussian beam with diameter σ at $1/e^2$ intensity, and fully coherent illumination [12]. In such a case, it has been shown that the intensity field presents a minimum lateral resolution (characterized here as the full width at half-maximum), $w_{\min} \approx 4.37\ a/[kA(n-1)]$, occurring at distance $f_0 = 54/125\ a^2/[A(n-1)]$, measured from the optical structure; k stands for the wavenumber $2\pi/\lambda$.

It is worth mentioning that the slope of the intensity on the optical axis, i.e., $dI(0,z)/dz$, has also been shown to be dependent on the input light beam diameter, σ. This effect, which has also been reported for axicons and lens axicons fabricated by other means [5,8], gives these optical structures additional functionalities, as the dynamic control of the intensity gradient along the optical axis by just using a dynamic iris, for instance, and also the possibility of keeping both the lateral resolution and the intensity practically constant within the focal region, as it occurs in the case of logarithmic axicons [5]. As already mentioned, all the details about the theoretical analysis of the optical field behind these particular optical structures obtained from a Lambertian evaporation source can be found in [12].

Continuing with the experimental report, Fig. 3 shows the spatial light-intensity distribution along the optical axis for a 4 mm diameter Gaussian cross section, 532 nm wavelength, input laser beam after passing through the deposit shown in Fig. 2. The spatial light-intensity distribution along the optical axis was recorded by means of a beam-profile analyzer based on a CCD (Newport, model LBP-2-USB), which was posted onto a linear translation stage with 25 mm travel (Newport, model M-423), and manual actuator with 1 μm precision (Newport, model SW-25). Snapshots were taken at different distances from the optical device, as indicated in the figure. Results show nondiffracting zero-order Bessel-type distributions in the output laser intensity, as expected for a Gaussian beam passing through an axicon.

On the other hand, the lateral resolution measured along the optical axis, within the focal region, is illustrated in Fig. 4(a) for the refractive optical structure of Fig. 2. A minimum lateral resolution of $w_{\min} \approx 37\ \mu$m, occurring around a distance $f_0 = 65$ mm, measured from the optical structure, is noticed in the plot, and it is to be mentioned that no changes in the lateral resolution have been detected when changing the input beam diameter.

The intensity profile along the optical axis has been derived from the spatial intensity distributions measured with the CCD from the color-coded images recorded. These data have been normalized with respect to the intensity at f_0, and they are plotted in Fig. 4(b). In this case, significant differences have been observed in these measurements when the input beam diameter, σ, was reduced by an iris [5]. Two illustrative sets of data for $\sigma = 2$ mm and $\sigma = 1$ mm are shown in this figure. As expected, values of the intensity have been observed to decrease at the end of the

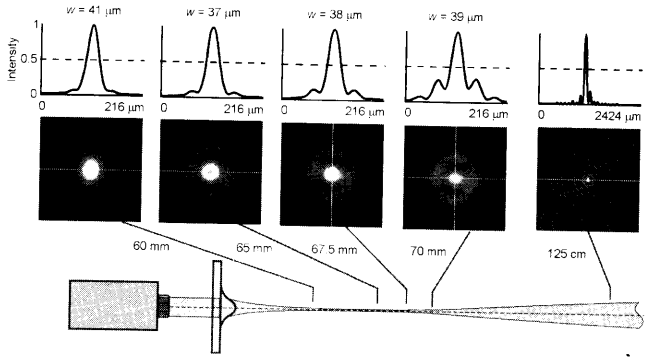

Fig. 3. (Color online) Spatial-intensity distribution behind the refractive optical structure of Fig. 2 at different distances on the optical axis, for 532 nm input laser radiation. Bessel-type curves are noticed in the intensity spatial distribution. Due to the characteristics of the beam-analyzer software, curves are normalized to the corresponding maximum intensity. Lateral resolutions within the focal region, measured from the curves, and dimensions of the image squared frames are indicated in micrometers.

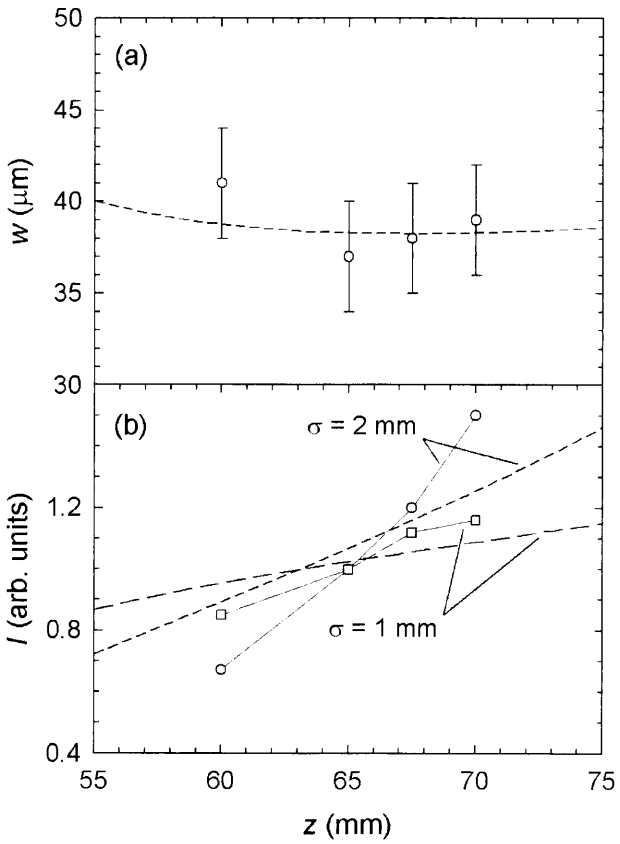

Fig. 4. (a) Lateral resolution and relative intensity for two different values of the (b) input beam diameter, measured through along the optical axis. Error bars in (a) have been derived from the Bessel curves derived from two perpendicular tracks (horizontal and vertical) on the corresponding 2D images illustrated in Fig. 3. Intensity values in (b) have been normalized with respect to the intensity at f_0 = 65 mm. Dashed curves in both figures are the theoretical values expected according to the theory described in [12]. Experimental points in (b) have been joined by thin curves for the sake of comparison with the theoretical curves.

focal region when energy couples diffraction orders higher than zeroth order.

Theoretical curves for the minimum lateral resolution, $w_{\min}$, and normalized intensity along the optical axis have also been plotted in Figs. 4(a) and 4(b), respectively. In general, there is observed to be a good agreement between theory and experiment, and differences are assumed to be mainly related to the intrinsic uncertainties of our experimental setup. Nevertheless, more research and better facilities are expected to throw light on the mechanisms, as well as on the optical performances of the optical structures fabricated according to the methodology introduced here.

Finally, it is worth noting that a value for the refractive index of $n = 2.6$, at 532 nm, has been estimated from the theoretical analysis of the experimental data, on the basis of the theory. This value is larger than the value of 2.3 reported for the same alloy prepared by both bulk and plasma-enhanced chemical vapor deposition. Keeping in mind the evidences of no changes in composition, this result supports a different structural scenario occurring in the deposits. More research is currently under development concerning the material characterization, and results will be given in due course.

In conclusion, differently from conventional milling and polishing techniques for optics fabrication, and also differently from expensive lithographic techniques imported from microelectronic technology [8], the present Letter probes the fabrication of these optical devices by cw laser effusion. The present results thus suggest an interesting way for the low-cost fabrication of axicons, and preliminary results of its demonstration are reported here. Due to this journal's manuscript-length restrictions, and keeping in mind that the aim of this Letter is to introduce to researchers in the field a new approach for the fabrication of axicons, more results will be given elsewhere.

This work has been partly supported by the Spanish Ministry of Education and Science through the National Physics I+D+i program (Spain), under the FIS2005-01409 project, and by the Regional Ministry of Innovation, Science and Enterprise of Andalusia, through the Excellence Research program, under the FQM-0654 project. J. A. Angel thanks the Regional Ministry for financial support.

References

1. D. B. Chrisey and G. K. Hubler, *Pulsed Laser Deposition of Thin Films* (Wiley, 1994).
2. M. N. R. Ashfold, F. Claeyssens, G. M. Fuge, and S. J. Henley, Chem. Soc. Rev. **33**, 23 (2004).
3. J. H. McLeod, J. Opt. Soc. Am. **44**, 592 (1954).
4. S. Y. Popov and A. T. Friberg, Appl. Opt. **7**, 537 (1998).
5. J. X. Pu, H. H. Zhang, and S. Nemoto, Opt. Eng. **39**, 803 (2000).
6. A. Burvall, K. Kolacz, Z. Jaroszewicz, and A. T. Friberg, Appl. Opt. **43**, 4838 (2004).
7. Z. Jaroszewicz, A. Burvall, and A. T. Friberg, Opt. Photon. News **16**(4), 34 (2005).
8. B. P. S. Ahluwalia, W. C. Cheong, X.-C. Yuan, L.-S. Zhang, S.-H. Tao, J. Bu, and H. Wang, Opt. Lett. **31**, 987 (2006).
9. J. M. González-Leal, J. A. Angel, P. Krecmer, E. Márquez, and R. Jiménez-Garay, Phys. Rev. B **74**, 205204 (2006).
10. R. Glang, in *Handbook of Thin Film Technology*, L. I. Maissel and R. Glang, eds. (McGraw-Hill, 1983).
11. D. R. Olander, Pure Appl. Chem. **62**, 123 (1990).
12. J. M. González-Leal, Opt. Express **15**, 5451 (2007).